

FT-Raman Spectroscopy as Diagnostic Tool of Congo Red Binding to Amyloids

VASSILIKI A. ICONOMIDOU,¹ GEORGIOS D. CHRYSIKOS,² VASSILIS GIONIS,² ANDREAS HOENGER,³ STAVROS J. HAMODRAKAS¹

¹ Department of Cell Biology and Biophysics, University of Athens, Panepistimiopolis, Athens 157 01, Greece

² Theoretical and Physical Chemistry Institute, National Hellenic Research Foundation, Athens 116 35, Greece

³ European Molecular Biology Laboratory, Meyerhofstrasse 1, Postfach 10.2209, D-69117 Heidelberg, Germany

Received 25 July 2002; revised 4 November 2002; accepted 5 November 2002

ABSTRACT: Chorion is the major component of silkmoth eggshell. More than 95% of its dry mass consists of the A and B families of low molecular weight structural proteins, which have remarkable mechanical and chemical properties protecting the oocyte and developing embryo from environmental hazards. We present data from FT-Raman spectroscopy of silkmoth chorion and amyloid-like fibrils formed from peptide analogues of chorion proteins, both unstained and stained by Congo red. The results show that FT-Raman spectroscopy is not a straightforward diagnostic tool for the specific interactions of Congo red with amyloids: a dilute aqueous solution of the Congo red dye at pH 5.5 and a thin solid film of the dye cast from this solution exhibit the same “diagnostic” Raman shifts relative to the neat Congo red dry powder as do amyloid fibrils formed from peptide analogues of chorion proteins stained by Congo red. An important consequence of this finding is that these shifts of the Raman active modes of Congo red are probably due to the formation of supramolecular dye aggregates in the presence of water. Therefore, this is not an appropriate diagnostic test for Congo red binding to amyloids. © 2003 Wiley Periodicals, Inc. *Biopolymers (Biospectroscopy)* 72: 185–192, 2003

Keywords: silkmoth chorion proteins; amyloid fibrils; electron microscopy; FT-Raman spectroscopy; Congo red binding

INTRODUCTION

Chorion, the major constituent (ca. 90%) of the eggshell of many insect and fish eggs, is an important biological structure with extraordinary mechanical and physiological properties.¹ The proteinaceous silkmoth chorion consists of more

than 200 different proteins, which account for more than 95% of its dry mass.¹ Silkmoth chorion proteins are variants of two major themes: they have been classified into two major classes, A and B.² Both families of silkmoth chorion proteins consist of three domains.³ The central domain is conserved in each class. The flanking N- and C-terminal domains are more variable and contain characteristic tandem repeats.³ Furthermore, the A and B central domains show distant similarities, suggesting that chorion genes constitute a superfamily derived from a single ancestral gene.⁴

Correspondence to: S. J. Hamodrakas (shamodr@cc.uoa.gr).
Contract grant sponsors: University of Athens; National Hellenic Research Foundation; EMBL Summer Visitors Program (to V.A.I. and S.J.H.).
Biopolymers (Biospectroscopy), Vol. 72, 185–192 (2003)
© 2003 Wiley Periodicals, Inc.

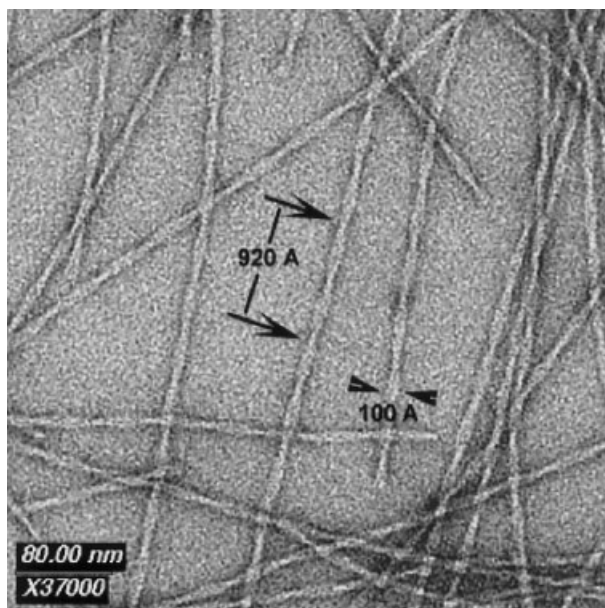


Figure 1. Electron micrograph of amyloid-like fibrils derived by self-assembly from a 9 mg mL^{-1} aqueous solution of the cA peptide at pH 5.5 (see text). The fibrils are negatively stained with 1% uranyl acetate. They are of indeterminate length (several microns), unbranched, and approximately 100 \AA in diameter and have a double helical structure. The pitch of the double helix is $\sim 920 \text{ \AA}$ (arrows). A pair of protofilaments (each $30\text{--}40 \text{ \AA}$ in diameter) are wound around each other, forming the double-helical fibrils. Scale bar = 800 \AA .

It was found to be very difficult to purify individual chorion proteins in large enough amounts of sufficient purity for structural studies. Therefore, in order to study chorion protein structural properties, we synthesized peptide analogues representative of parts or the entire central conservative domain of the two silkmoth chorion protein families (A and the B).⁵ The synthesis of such peptides was made because the central domains of the A and B families of chorion proteins are highly conserved in both sequence and length, and this conservation most probably indicates that these domains play an important functional role in the formation of silkmoth chorion structure.⁶

We have recently shown that peptide analogues, both of the entire central domain of the A family of silkmoth chorion proteins (cA peptide) and a part of the central domain of the B family of silkmoth chorion proteins (B peptide), form amyloid-like fibrils by self-assembly mechanisms under a great variety of conditions *in vitro*.^{7,8} The fibrils, $\sim 100 \text{ \AA}$ in diameter (Fig. 1), bind Congo

red and show the red-green birefringence characteristic for amyloids, when seen under crossed polars (data not shown). Suspensions of these fibrils form oriented fibers, which give characteristic “cross- β ”-X-ray diffraction patterns,⁷ a characteristic feature of amyloids as well (see Iconomidou et al.^{7,8} and references therein). These data, combined with the fact that silkmoth chorion consists of fibrils similar in appearance to the amyloid fibrils formed from peptide analogues of parts of chorion proteins and structural data of silkmoth chorion presented elsewhere,⁷ probably suggest that silkmoth chorion is a natural, protective amyloid that is important for the survival and development of the oocyte and the developing embryo.^{7,8} This role is in contrast to that of amyloids associated with serious diseases including Alzheimer’s disease, transmissible spongiform encephalopathies, type II diabetes mellitus, and a number of systemic polyneuropathies.^{9–12}

Recently, IR, FT-Raman and UV spectroscopy were used to study the binding of Congo red to deposits of Alzheimer’s amyloid in cerebral tissue and other typical β -amyloid proteins.¹³ Several Raman features attributed to Congo red were found to shift upon amyloid binding, and Raman spectroscopy has therefore been considered a powerful diagnostic tool for β -amyloids. In this work we present the FT-Raman spectra of silkmoth chorion, a solid and robust structure consisting of proteins adopting an antiparallel β -sheet type of structure, a naturally designed protective amyloid,^{6,7} as well as cA peptide amyloid-like fibrils, both unstained and stained with Congo red. Contrary to earlier reports, we provide evidence that the FT-Raman spectra of the stained samples do not provide unequivocal evidence for an amyloid-specific binding of Congo red.

MATERIALS AND METHODS

Formation of Amyloid-Like Fibrils, Formation of Oriented Fibers, and Preparation of Silkmoth Chorion Samples

A cA peptide analogue of the central domain of silkmoth chorion A proteins was dissolved in doubly distilled water (pH 5.5) at a concentration of 9 mg/mL to produce amyloid-like fibrils after 3–4 weeks of incubation. Oriented fibers, suitable for X-ray diffraction, were obtained from suspensions of cA peptide amyloid-like fibrils as described in

Iconomidou et al.⁷ Clean samples of contaminant-free silkworm chorions and silkworm chorion fragments were obtained as described in Hamodrakas et al.¹⁴

Negative Staining

For negative staining, cA peptide fibril suspensions were applied to glow-discharged 400-mesh carbon coated copper grids for 60 s. The grids were (occasionally) flash-washed with $\sim 150 \mu\text{L}$ of distilled water and stained with a drop of 1% (w/v) aqueous uranyl acetate for 45 s. Excess stain was removed by blotting them with filter paper, and then they were air dried. The grids were examined in a Philips CM120 Biotwin transmission electron microscope operating at 100 kV. Photographs were obtained by a retractable slow scan CCD camera (SSCTM, Gatan Inc.) utilizing the Digital Micrograph 2.5.8 program (Gatan Inc.).

Congo Red Staining and Polarized Light Microscopy

A cA peptide fiber used for X-ray diffraction studies (which was prepared from a suspension of cA amyloid-like fibrils and produced very rich, oriented cross- β X-ray diffraction patterns as described in Iconomidou et al.⁷) was stained with a 10 mM Congo red (Sigma) solution in phosphate buffered saline (PBS, pH 7.4) for approximately 2 h (after the X-ray exposures). It was then washed several times with 90% ethanol and left to dry. Subsequently, the fiber was observed under bright field and between crossed polars utilizing a Zeiss KL 1500 polarizing stereomicroscope equipped with an MC 80 DX camera.

Hemispherical half-chorions^{14,15} or approximately flat chorion fragments were stained with a Congo red solution as above for several hours under reducing conditions in the dark. They were then washed thoroughly with 90% ethanol and left to dry.

FT-Raman Spectroscopy

For the Raman measurements the following types of samples were used:

1. cA amyloid fibrils (a drop of a 10 μL suspension of cA peptide fibrils was cast on a front coated Au mirror and left to dry);
2. an oriented fiber of the cA peptide, used as a sample for X-ray diffraction measurements, stained with Congo red (as described in the staining by Congo red procedure above);
3. silkworm chorions of the wild-type moth *Au-theraea polyphemus*;
4. silkworm chorions of the wild-type moth *A. polyphemus* stained with Congo red (as described in the staining by Congo red procedure above);
5. Congo red as supplied from Sigma (dry powder);
6. aqueous solutions of Congo red (10 mM, pH 5.5) and Congo red dissolved (10 mM) in PBS (pH 7.4); and
7. thin films of Congo red cast on an aluminum foil from aqueous solutions (10 mM, pH 5.5).

Raman spectra were obtained on a Fourier transform instrument (Bruker RFS 100) employing for excitation ca. 400-mW of a Nd:YAG 1064-nm line in backscattering geometry. Excitation in the near IR greatly reduces the fluorescence of the proteinaceous samples and eliminates the need for prolonged laser annealing, which is necessary if excitation in the visible is employed instead. The resolution was 4 cm^{-1} and the total acquisition time was 10 h (about 10,000 scans). The interferograms were Fourier transformed in 1-h acquisition time segments in order to enable the detection of time dependent phenomena (sample degradation, luminescence, bleaching, etc.). Subsequently, the spectra were averaged and the standard deviation (σ) was calculated. The spectra of the nonproteinaceous samples were also measured at 4 cm^{-1} resolution, but with about 400 scans.

Postrun Computations of Spectra

The Raman scattering peak maxima were determined from the minima in the second derivative of the corresponding spectra. Derivatives were computed analytically using routines of Bruker OPUS/Windows 2000 software and included smoothing by the Savitzky–Golay algorithm over a 4 cm^{-1} range around each data point.¹⁶ Smoothing over narrower ranges resulted in a deterioration of the signal to noise ratio and did not increase the number of minima that could be determined with confidence.

RESULTS AND DISCUSSION

Figure 1 shows amyloid-like fibrils derived by self-assembly from a 9 mg/mL aqueous solution of

the cA peptide analogue of silkmoth chorion proteins (pH 5.5) after negative staining.

Figure 2 shows the FT-Raman spectrum of cA peptide amyloid-like fibrils shown in Figure 1 but cast on an Au front mirror. The FT-Raman spectrum of an oriented fiber derived from a suspension of cA peptide amyloid-like fibrils and stained with the dye Congo red is shown in Figure 3. This fiber was used to obtain rich, oriented cross- β X-ray diffraction patterns. These, together with supporting evidence from electron microscope studies (Fig. 1) and red-green birefringence under crossed polars after Congo red staining (data not shown), indicate the amyloid-like nature of cA peptide fibrils.⁷

Figure 4 shows the FT-Raman spectrum of an intact chorion sample from the wild-type silkmoth *A. polyphemus*. Figure 5 displays the FT-Raman spectrum of the same chorion sample stained with Congo red.

The bands observed in these FT-Raman spec-

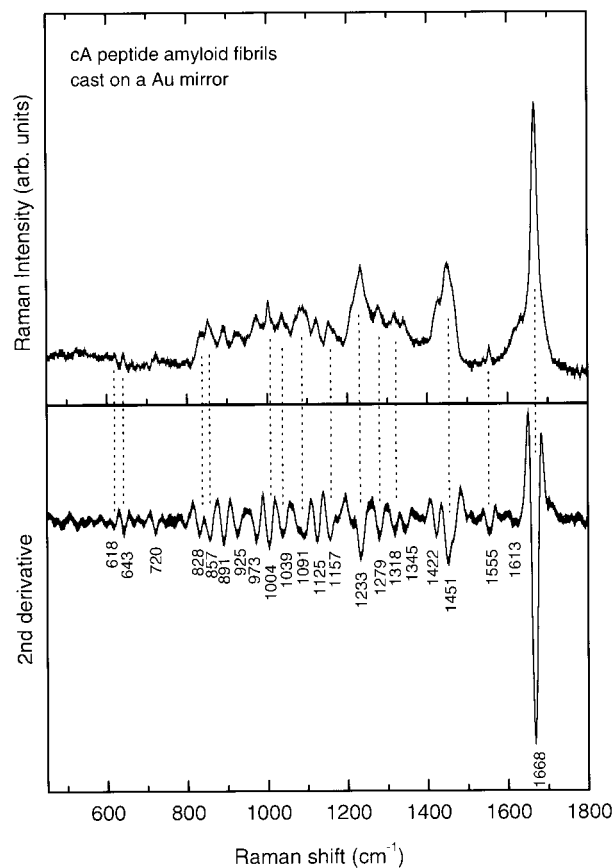


Figure 2. The FT-Raman (450–1800 cm^{-1}) spectrum of cA peptide amyloid fibrils cast on a gold mirror. A second derivative spectrum is included. Error bar = 0.5σ .

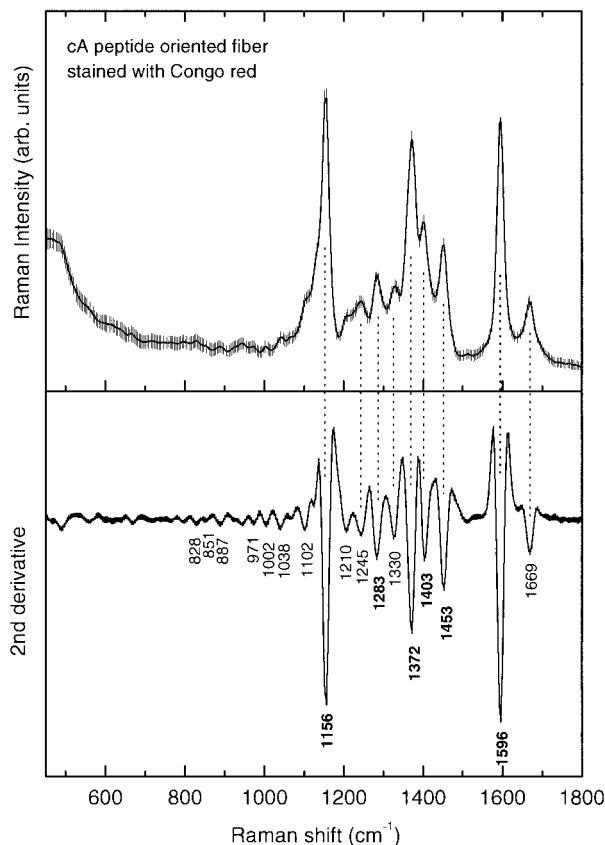


Figure 3. The FT-Raman (450–1800 cm^{-1}) spectrum of an oriented fiber produced from a suspension of cA peptide amyloid fibrils stained with Congo red. Second derivative spectra are included. Error bar = 0.5σ .

tra (exact locations determined from the second derivative spectra) are compiled in Table I, along with tentative assignments.^{17–21}

In both unstained and stained materials the position of the amide I ($\sim 1670 \text{ cm}^{-1}$) and III ($\sim 1230 \text{ cm}^{-1}$) bands in the Raman spectra are well-known indicators of β -sheet secondary structure. These β sheets are judged to be antiparallel, especially from the presence of a band (seen as a shoulder) at $\sim 1691 \text{ cm}^{-1}$ in the corresponding attenuated total reflectance FTIR spectra (data not shown) of the same materials.^{2,8,22–24} This evidence is clearly in agreement with our earlier investigations of the structure of the cA peptide amyloid fibrils and cA peptide oriented fiber from X-ray diffraction, Raman, and IR data and modeling studies.⁷ It also confirms the structure of silkmoth chorion proteins from conventional Raman spectroscopy studies conducted 20 years ago,¹⁵ which indicate that silkmoth chorion proteins and peptides adopt a “cross- β -sheet” type of

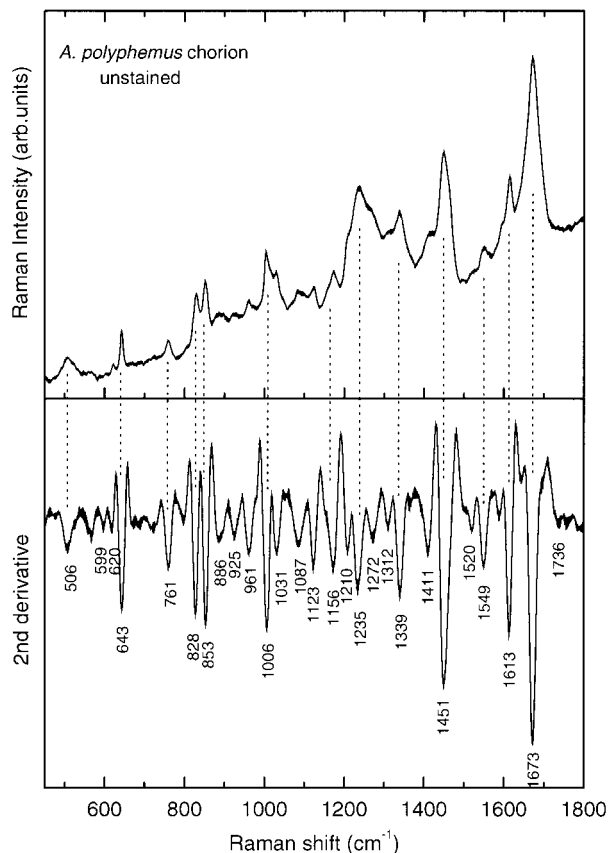


Figure 4. The FT-Raman ($450\text{--}1800\text{ cm}^{-1}$) spectrum of a silkworm chorion of *A. polyphemus*. Second derivative spectra are included. Error bar = 0.5σ .

structure (see also Hamodrakas et al.⁶ and references therein).

Comparing the Raman spectra of the unstained cA peptide organized into amyloid-like fibrils to those of the lyophilized cA from Benaki et al.⁵ reveals that the organization results in considerably sharper and better resolved amide I and III features. The width at half-maximum intensity of the main Raman amide I feature is about 50 cm^{-1} in the lyophilized cA,⁵ but it drops to 21 cm^{-1} in its organized unstained form. It is interesting that the bandwidth of the same feature in the Raman spectrum of the unstained silkworm chorion (Fig. 4) is about 27 cm^{-1} (i.e., indicative of rather strong organization and the presence of uniform β -sheet structures; see also Hamodrakas et al.¹⁵).

Furthermore, the FT-Raman spectra (Figs. 2–5) contain useful information about the state of several amino acid residues of silkworm chorion proteins and peptides (Table I), which will not be discussed here.

Instead, we wish to draw particular attention to the binding of the Congo red dye to cA peptide fibrils and to the silkworm chorion itself and discuss its implications.

A comparison of the Raman spectra of the unstained and stained cA peptide amyloid fibrils (Figs. 2 and 3, respectively) indicates that the latter contains strong features at 1596 , 1453 , 1403 , 1372 , and 1156 cm^{-1} that are not present in the former. These features are clearly due to the spectroscopic signature of the Congo red dye. The strongest amide I band in the Raman spectrum of the stained cA peptide amyloid fibrils appears to be about 4 times weaker than its neighboring 1596 cm^{-1} Congo red mode (Fig. 3). The Congo red modes in the Raman spectrum of the stained silkworm chorion are less pronounced (presumably because the ratio of the chorion protein to Congo red is much larger in this case) than those of the stained cA sample. Nevertheless, they can

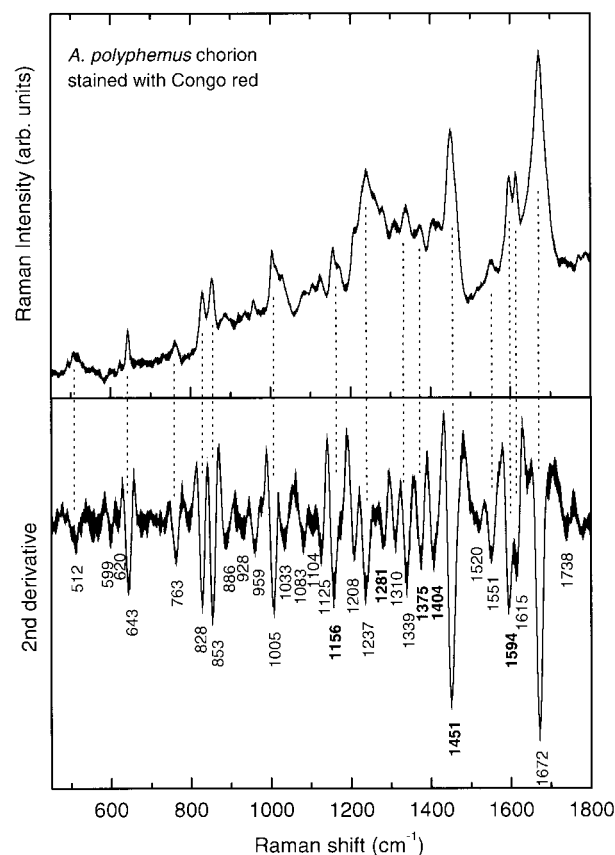


Figure 5. The FT-Raman ($450\text{--}1800\text{ cm}^{-1}$) spectrum of a silkworm chorion of *A. polyphemus* stained with Congo red. A second derivative spectrum is included. Error bar = 0.5σ .

Table I. Main Raman (450–1800 cm^{-1}) Peak Maxima of cA Peptide Amyloid Fibrils Cast on Au Mirror, Fiber Produced from Suspension of cA Peptide Amyloid Fibrils Stained with CR, Silkmoth Chorion of *A. polyphemus*, and Silkmoth Chorion of *A. polyphemus* Stained with CR and Their Tentative Assignments

Cast cA Peptide Amyloid Fibrils	cA Peptide Fiber Stained with CR	Silkmoth Chorion	Silkmoth Chorion Stained with CR	Assignments
		1736	1738	—COOH
1668	1669	1673	1672	β sheet
1613		1613	1615	Tyr, Phe
	1596		1594	CR
1555		1549	1551	Amide II
		1520	1520	Amide II
1451		1451		CH_2 deformation
	1453		1451	CR
1422		1411		CH_2 deformation
	1403		1404	CR
	1372		1375	CR
1345	1330	1339	1339	CH deformation
1318		1312	1310	CH deformation
1279		1272		β turns? coil?
	1283		1281	CR
1233	1245	1235	1237	β sheet
	1210	1210	1208	Tyr, Phe
1157		1156		
	1156		1156	CR
1125		1123	1125	C—N stretching
	1102		1104	C—N stretching
1091		1087	1083	
1039	1038	1031	1033	Phe
1004	1002	1006	1005	Phe
973	971	961	959	
925		925	928	C—C stretching
891	887	886	886	Trp
857	851	853	853	Tyr
828	828	828	828	Tyr
		761	763	Trp
720				
643		643	643	Tyr, Phe
618		620	620	Phe
		599	599	
		506	512	S—S stretching

CR, Congo red. The values in bold represent Congo red modes.

be clearly observed at the same frequencies in the second derivative spectra (Fig. 5).

Recently, Sajid et al.¹³ reported that Congo red exhibits significant shifts of its Raman active modes when bound to β -amyloid peptides or Alzheimer's disease brain tissue. They claimed that the shifts of the stretching mode of the azomoiety from 1353 (powder) to 1374 cm^{-1} (amyloid), a smaller shift of the phenyl ring mode from 1589 to 1594 cm^{-1} , and the appearance of a feature at about 1401 cm^{-1} are of major diagnostic impor-

tance. Remarkably, our spectra of both the stained cA fiber and silkmoth chorion (Figs. 3 and 5) exhibit the Congo red bands shifted in the manner and extent reported by Sajid et al.,¹³ and this appears at first sight to provide additional strong evidence for their amyloid structure.

However, given the fact that the interactions between Congo red and the protein β sheets are not yet fully understood at (or near) the atomic level and that there is still doubt whether Congo red is an amyloid-specific dye,^{25–27} we proceeded

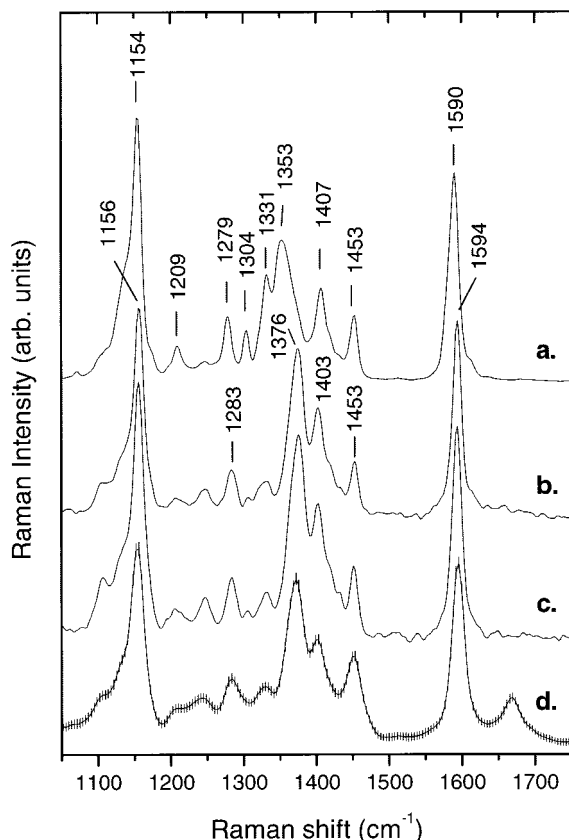


Figure 6. FT-Raman spectra ($1000\text{--}1800\text{ cm}^{-1}$) of (a) Congo red powder (Sigma), (b) a Congo red aqueous solution (10 mM, pH 5.5), (c) a thin film cast on Al foil from the aqueous solution of Congo red, and (d) an oriented fiber produced from a suspension of cA peptide amyloid fibrils stained with Congo red (Fig. 3). Error bar = 0.5σ .

to study its Raman spectra in dilute aqueous solutions and film casts.

Surprisingly, our spectra (Fig. 6) indicate that the stained cA fiber, a dilute aqueous solution at pH 5.5, and a thin solid film of the dye cast from this solution exhibit the same Raman spectra, which are, within the resolution of the experiment, identical to the spectra of Sajid et al.¹³ but differ from that of the neat Congo red powder. The important consequence of this finding is that these shifts of the Raman active modes of Congo red are probably due to the formation of supramolecular dye aggregates in the presence of water.²⁸ They originate from the π interactions of the highly polarizable conjugated central parts of the dye molecules and not from any specific binding to the proteinaceous substrate, regardless of whether this is amyloid or not. FT-Raman spectroscopy, despite its advantages in elucidating the

secondary structure of proteins, does not provide evidence for an amyloid-specific binding of Congo red.

CONCLUSION

FT-Raman spectroscopy has been used successfully to determine the secondary structure of silkworm chorion proteins and chorion protein peptide analogues forming amyloid-like fibrils, both unstained and stained by Congo red. However, and contrary to earlier reports, when applied to stained specimens it does not detect any specific interactions of amyloid-like fibrils with the Congo red dye.

The authors are grateful for the financial support of this work by the University of Athens and the National Hellenic Research Foundation. The first and fifth authors (V.A.I and S.J.H.) acknowledge the help of the EMBL Summer Visitors Program. We thank the referees of this article for useful comments.

REFERENCES

1. Kafatos, F. C.; Regier, J. C.; Mazur, G. D.; Nadel, M. R.; Blau, H. M.; Petri, W. H.; Wyman, A. R.; Gelinis, R. E.; Moore, P. B.; Paul, M.; Efstratiadis, A.; Vournakis, J. N.; Goldsmith, M. R.; Hunsley, J. R.; Baker, B.; Nardi, J.; Koehler, M. In *Results and Problems in Cell Differentiation*; Beerman, W., Ed.; Springer-Verlag: New York, 1977; pp 45–145.
2. Regier, J. C.; Kafatos, F. C. In *Comprehensive Insect Biochemistry, Physiology and Pharmacology*; Gilbert, L. I., Kerkut, G. A., Eds.; Pergamon: New York, 1985; pp 113–151.
3. Hamodrakas, S. J.; Jones, C. W.; Kafatos, F. C. *Biochim Biophys Acta* 1982, 700, 42–51.
4. Lekanidou, R.; Rodakis, G. C.; Eickbush, T. H.; Kafatos, F. C. *Proc Natl Acad Sci USA* 1986, 83, 6514–6518.
5. Benaki, D. C.; Aggeli, A.; Chryssikos, G. D.; Yianopoulos, Y. D.; Kamitsos, E. I.; Brumley, E.; Case, S. T.; Boden, N.; Hamodrakas, S. J. *Int J Biol Macromol* 1998, 23, 49–59.
6. Hamodrakas, S. J. In *Results and Problems in Cell Differentiation*; Case, S. T., Ed.; Springer-Verlag: Berlin, 1992; pp. 115–186.
7. Iconomidou, V. A.; Vriend, G.; Hamodrakas, S. J. *FEBS Lett* 2000, 479, 141–145.
8. Iconomidou, V. A.; Chryssikos, G. D.; Gionis, V.; Vriend, G.; Hoenger, A.; Hamodrakas, S. J. *FEBS Lett* 2001, 499, 268–273.
9. Pepys, M. B. In *The Oxford Textbook of Medicine*,

- 3rd ed.; Weatherall, D. J., Ledingham, J. G. G., Warell, D. A., Eds.; Oxford University Press: Oxford, UK, 1996; pp 1512–1524.
10. Kelly, J. F. *Curr Opin Struct Biol* 1996, 6, 11–17.
 11. Kelly, J. F. *Curr Opin Struct Biol* 1998, 8, 101–106.
 12. Dobson, C. M. *Trends Biochem Sci* 1999, 24, 329–332.
 13. Sajid, J.; Elhaddaoui, A.; Turrel, S. *J Mol Struct* 1997, 408/409, 181–184.
 14. Hamodrakas, S. J.; Paulson, J. R.; Rodakis, G. C.; Kafatos, F. C. *Int J Biol Macromol* 1983, 5, 149–153.
 15. Hamodrakas, S. J.; Asher, S. A.; Mazur, G. D.; Regier, J. C.; Kafatos, F. C. *Biochim Biophys Acta* 1982, 703, 216–222.
 16. Savitsky, A.; Golay, M. J. E. *Anal Chem* 1964, 36, 1627–1639.
 17. Frushour, B. J.; Koenig, J. L. In *Advances in Infrared and Raman Spectroscopy*; Clark, R. J. H., Hester, R. E., Eds.; Heyden: London, 1975; pp 35–97.
 18. Yu, N. T. *Crit Rev Biochem* 1977, 4, 229–280.
 19. Spiro, T. G.; Gaber, B. P. *Annu Rev Biochem* 1977, 46, 553–572.
 20. Bandekar, J.; Krimm, S. *Proc Natl Acad Sci USA* 1979, 76, 774–777.
 21. Carey, P. R. In *Biochemical Applications of Raman and Resonance Raman Spectroscopies*; Academic: New York, 1982.
 22. Haris, P. I.; Chapman, D. *Biopolym (Pept Sci)* 1995, 37, 251–263.
 23. Jackson, M.; Mantsch, H. H. *Crit Rev Biochem Mol Biol* 1995, 30, 95–120.
 24. Iconomidou, V. A.; Chryssikos, D. G.; Gionis, V.; Pavlidis, M. A.; Paipetis, A.; Hamodrakas, S. J. *J Struct Biol* 2000, 132, 112–122.
 25. Turnell, W. G.; Finch, J. T. *J Mol Biol* 1992, 227, 1205–1223.
 26. Carter, D. B.; Chou, K. C. *Neurobiol Aging* 1998, 19, 37–40.
 27. Khurana, R.; Uversky, V. N.; Nielsen, L.; Fink, A. L. *J Biol Chem* 2001, 276, 22715–22721.
 28. Skowronek, M.; Stopa, B.; Konieczny, L.; Rybarska, J.; Piekarska, B.; Szneler, E.; Bakalarski, G.; Roterman, I. *Biopolymers* 1998, 46, 267–281.